AD-A117 806 RENSSELAER POLYTECHNIC INST TROY NY DEPT OF MATHEMAT--ETC F/G 20/4
NEW HIGHER-ORDER BOUNDARY-LAYER EQUATIONS FOR LAMINAR AND TURBU--ETC(U)
APR 82 C KLEINSTREUER, A EGLIMA, J E FLAHERTY AFOSR-80-0192

UNCLASSIFIED AFOSR-TR-82-0588 NL

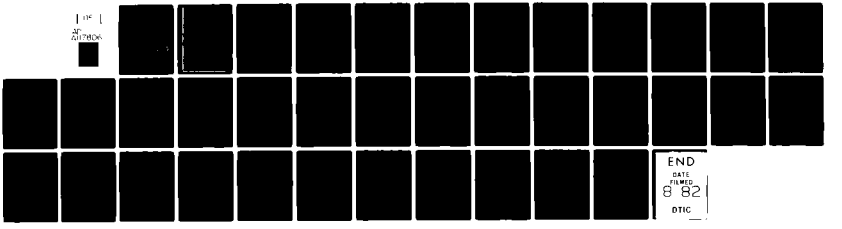

UNCLASSIFIED

SECURITY CLASSIFICATION OF THIS PAGE (When Data Entered)

REPORT DOCUMENTATION PAGE	READ INSTRUCTIONS BEFORE COMPLETING FORM
1. REPORT NUMBER **AFOSR-TR- 82-0588**	2. GOVT ACCESSION NO
3. RECIPIENT'S CATALOG NUMBER	
4. TITLE (and Subtitle) NEW HIGHER-ORDER BOUNDARY-LAYER EQUATIONS FOR LAMINAR AND TURBULENT FLOW PAST AXISYMMETRIC BODIES	5. TYPE OF REPORT & PERIOD COVERED TECHNICAL
	6. PERFORMING ORG. REPORT NUMBER
7. AUTHOR(s) C. Kleinstreuer, A. Eglima, and J.E. Flaherty	8. CONTRACT OR GRANT NUMBER(s) AFOSR-80-0192
9. PERFORMING ORGANIZATION NAME AND ADDRESS Department of Mathematical Sciences Rensselaer Polytechnic Institute Troy NY 12181	10. PROGRAM ELEMENT, PROJECT, TASK AREA & WORK UNIT NUMBERS PE61102F; 2304/A2
11. CONTROLLING OFFICE NAME AND ADDRESS Mathematical & Information Sciences Directorate Air Force Office of Scientific Research Bolling AFB DC 20332	12. REPORT DATE APR 82
	13. NUMBER OF PAGES 36
14. MONITORING AGENCY NAME & ADDRESS(if different from Controlling Office)	15. SECURITY CLASS. (of this report) UNCLASSIFIED
	15a. DECLASSIFICATION/DOWNGRADING SCHEDULE

16. DISTRIBUTION STATEMENT (of this Report)

Approved for public release; distribution unlimited.

17. DISTRIBUTION STATEMENT (of the abstract entered in Block 20, if different from Report)

DTIC ELECTE AUG 0 4 1982 S D E

18. SUPPLEMENTARY NOTES

Submitted to SIAM J. Applied Mathematics.

19. KEY WORDS (Continue on reverse side if necessary and identify by block number)

Boundary layer flows, curvature effects, separation, axisymmetric bodies.

20. ABSTRACT (Continue on reverse side if necessary and identify by block number)

New sets of boundary-layer equations accounting for flow field non-uniformities such as curvature effects, normal stress and pressure variations as well as separation, are derived. The boundary-layer flow domain is subdivided into (1) a parabolic region where the fluid flow is approximately parallel to the submerged body, i.e., $v \ll u$ and (2) an elliptic region which includes the line of separation where significant interactions between the boundary-layer and the outer potential flow occur, i.e., $v \approx u$. Closure for the turbulent flow equations has to be obtained with submodels for the Reynolds stresses which (CONTINUED)

DD FORM 1 JAN 73 1473 EDITION OF 1 NOV 65 IS OBSOLETE

82 08 03 115

UNCLASSIFIED

SECURITY CLASSIFICATION OF THIS PAGE (When Data Entered)

AD A117806

DTIC FILE COPY

ITEM #20, CONTINUED: reflect the effects of boundary-layer thickening as well as separation. The accuracy of the parabolic equations was compared with Van Dyke's higher-order boundary-layer equations for laminar flow past a body with longitudinal curvature. The results demonstrate that the new modeling equations make a measurable difference as expected from observations made by Bradshaw and others.

AFOSR-TR- 82-0588 SIAM J. on Appl. Math
April 1982

NEW HIGHER-ORDER BOUNDARY-LAYER EQUATIONS FOR LAMINAR AND TURBULENT FLOW PAST AXISYMMETRIC BODIES

C. KLEINSTREUER*, A. EGHLIMA** AND J.E. FLAHERTY†
Rensselaer Polytechnic Institute
Troy, NY 12181

Abstract. New sets of boundary-layer equations accounting for flow field non-uniformities such as curvature effects, normal stress and pressure variations as well as separation, are derived. The boundary-layer flow domain is subdivided into (1) a parabolic region where the fluid flow is approximately parallel to the submerged body, i.e. $v \ll u$ and (2) an elliptic region which includes the line of separation where significant interactions between the boundary-layer and the outer potential flow occur, i.e. $v \approx u$. Closure for the turbulent flow equations has to be obtained with submodels for the Reynolds stresses which reflect the effects of boundary-layer thickening as well as separation. The accuracy of the parabolic equations was compared with Van Dyke's higher-order boundary-layer equations for laminar flow past a body with longitudinal curvature. The results demonstrate that the new modeling equations make a measurable difference as expected from observations made by Bradshaw and others.

1. Introduction. An accurate but also computationally efficient description of internal or external, laminar and turbulent flow fields is important for the optimal design of a variety of mechanical systems. For example, simulation of the proposed boundary-layer equations can aid in improving the design of bent diffusors and submerged bodies in terms of reduced pressure loss and total drag reduction respectively. Furthermore, propeller performance of marine crafts could be enhanced with a more accurate prediction of the velocity field in the near-wake region.

At the high Reynolds numbers of interest, the analysis involves the usual difficulties encountered with turbulent boundary layers in a pressure

*Department of Chemical and Environmental Engineering.
**Department of Mechanical Engineering.
†Department of Mathematical Sciences. The work of this author was partially sponsored by the U.S. Air Force Office of Scientific Research, Air Force Systems Command, USAF, under Grant Number AFOSR-80-0191. The United States Government is authorized to reproduce and distribute reprints for government purposes notwithstanding any copyright notation thereon.

gradient now accentuated by the boundary layer thickness (relative to the transverse and/or longitudinal body radius) and eventually the effects of flow separation. Van Dyke (1962, 1969) has shown, that transverse curvature makes a contribution to differential and integral flow parameters that is additive to that of longitudinal curvature and of the same relative order. Meroney and Bradshaw (1975) have measured turbulent boundary layer growth in a prolonged bend and show that a small (one percent) change in the curvature of a convex surface produces a relatively large (ten percent) change in the integral properties of the flow field, such as total drag. Further measurements of curvature effects on laminar and turbulent boundary-layer flow parameters were published by Huang et al. (1980), Gillis and Johnson (1980), Smith et al. (1979), Patel and Lee (1978), Ramaprian and Shivaprasd (1978), and Patel (1974). Different investigators (e.g. Rastogi and Whitelaw (1971), Bradshaw (1973, 1975), Patel and Lee (1978), Granville (1978), Cebeci et al. (1978), Huang et al. (1979), Cebeci (1979), and Patel and Choi (1980)) have used or described different methods to solve thick boundary layer problems for special situations by taking into account some of the non-uniformities, such as longitudinal curvature or transverse curvature effects, but not all of them as discussed earlier. On the other hand we will show in subsequent sections that the equation usually employed for calculating the longitudinal curvature effect (Van Dyke (1969)) is not complete. Our derivations (Sections 3 & 5) indicate that additional terms of the same order of magnitude as Van Dyke's second order terms are necessary for representing the influence of longitudinal curvature on the growth of boundary layers. Authors (e.g. Cebeci (1971), Rastogi and Whitelaw (1971), Cebeci et al. (1978, (1979)) who employed a turbulent version of Van Dyke's equation could not predict the curvature effects on integral properties of

the flow field as measured by Meroney and Bradshaw (1975). Solutions of the boundary layer equations employing prescribed variations of the pressure gradient (Patel (1974)) failed near the point of flow separation and consequently a singular behavior in the boundary layer solution was postulated (Goldstein (1948)). However, Williams (1977) used the results of various researchers (e.g. Keller and Takami (1966), Son and Hanratty (1969), Dennis (1970), and Masliyah (1970)), who solved the Navier-Stokes equation for flows that include the point of zero stress, to show that such a singular behavior is not a physical property of the flow but it is a characteristic of the solutions of the boundary layer equations.

We are presenting higher-order boundary-layer equations that simulate incompressible laminar and turbulent flow fields more accurately than with existing models.

2. System conceptualization and approach. Consider the steady two-dimensional or axisymmetric flow of a Newtonian fluid past a stationary body. Figure 1 schematically depicts the various flow developments including the three major regions of interest at the tail of the submerged body where the boundary layer is thick due to curvature effects. In region I the mean flow streamlines remain nearly parallel to the solid surface regardless of the relative thickness of the boundary layer. In region II streamlines are not parallel to the body surface and the velocity component u parallel to the body surface is of the same order of magnitude as the velocity component v normal to the body. The flow in this region is characterized by strong interactions between the boundary layer and the outer inviscid flow in region III. Basically two new sets of governing equations for thick turbulent

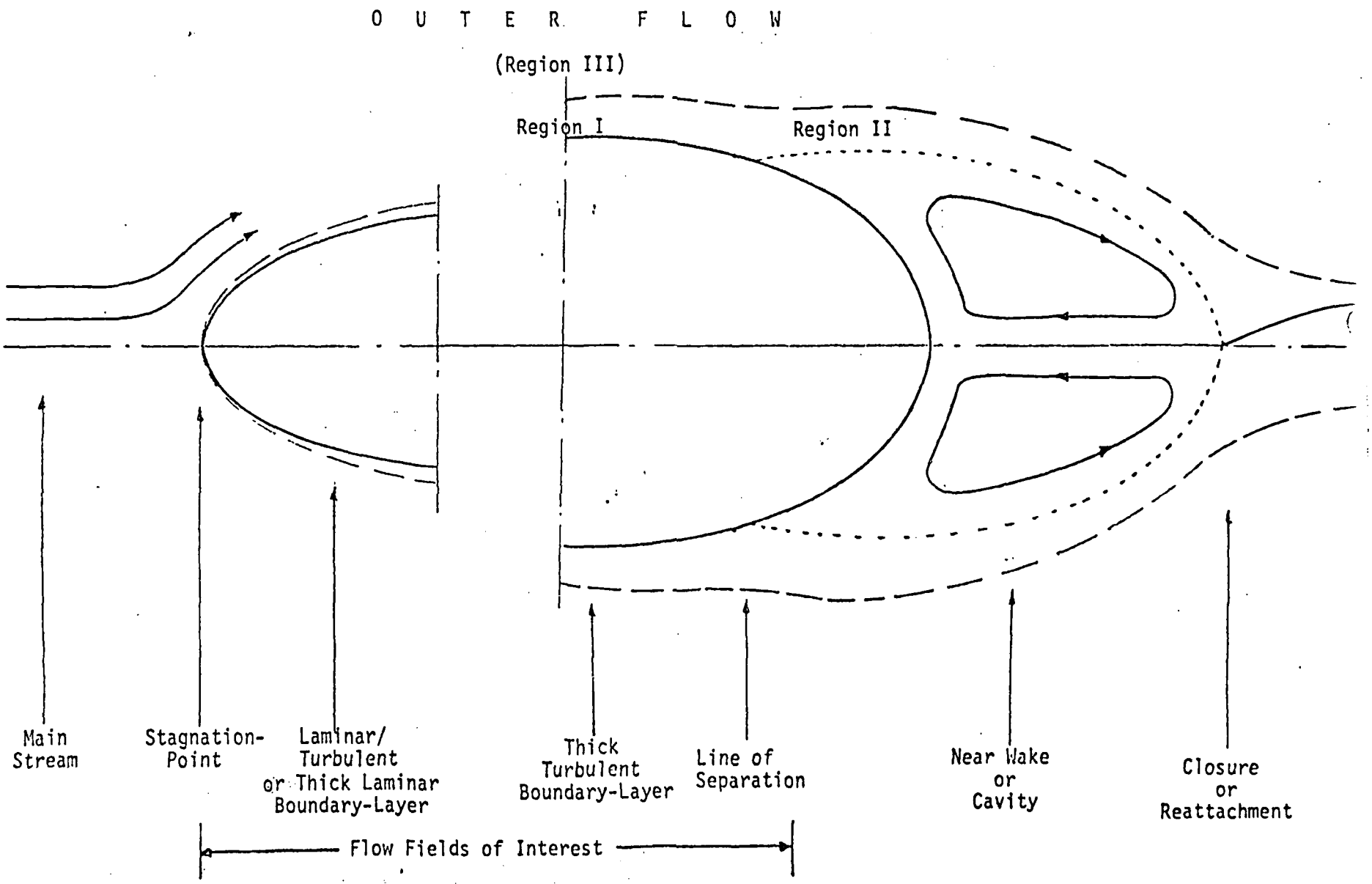

Figure 1: Schematics of Flow Domain

boundary layer flows (regionI and II) are derived. Laminar flow fields with any type of curvature effect can be regarded as a special case of the first complete set of modeling equations.

The approach for simulating a general external or internal flow system is best illustrated with reference to Fig. 1. Starting from the stagnation point, a suitable computer code (e.g. Cebeci et al.(1978)) is employed until the boundary layer becomes thick, i.e. $\frac{\delta}{R} << 1$ is not valid any more. The intermediate results are then relayed to the program of our new parabolic equations for region I which are accurate as long as $v << u$ which may include the point of separation. We note that boundary layer thickening might occur for certain body geometries at quite an early stage as demonstrated in Section 6 for a laminar flow case study. When reverse flow occurs and $v \approx u$, the new elliptic modeling equations of region II are activated. Interaction with the potential flow (Cebeci et al. (1978)) is simulated with the local displacement thickness using an iterative procedure. In order to preserve computational efficiency, a continuous function is assumed for the pressure drop from the calculated pressure at the separation point to the wake pressure behind the afterbody which is apparently of the order of magnitude of the outer flow pressure. The near-wake velocity field is then actually computed with Schlichting's solution for (circular) wakes behind a three-dimensional body (e.g. White (1974), Riley and Metcalfe (1980)). More detailed investigations for wake flow are discussed by Wu (1972), Pope and Whitelaw (1976) and recently by Smith (1979).

3. Derivation of the governing equations for region I. The governing equations for the generalized class of thick boundary layer developments are written in terms of fluid mass and momentum fluxes (cf. Kleinstreuer (1982)):

$$\frac{\partial \rho}{\partial t} + \underset{\sim}{\nabla}\cdot\rho\underset{\sim}{v} = 0 \tag{3.1}$$

$$\frac{\partial}{\partial t}\rho\,\underset{\sim}{v} + \underset{\sim}{\nabla}\cdot\rho\underset{\sim}{v}\,\underset{\sim}{v} = -\,\underset{\sim}{\nabla}\cdot\underset{\sim}{\pi} + \rho\underset{\sim}{f} \tag{3.2}$$

where $\rho\underset{\sim}{v}$ is the mass flux (i.e., fluid mass per unit area and per unit time), $\rho\underset{\sim}{v}\underset{\sim}{v}$ is the momentum flux and $\underset{\sim}{\pi} \equiv p\underset{\sim}{\delta} + \underset{\sim}{\tau}$ is the total stress tensor consisting of the thermodynamic pressure as well as shear plus normal stresses.

We restrict our analysis to the steady two-dimensional or axisymmetric flow of a Newtonian fluid around a submerged body and introduce the tangential and normal (s, n) orthogonal coordinate system shown in Fig. 2. Under these conditions, the equations of continuity and momentum may be written as:

$$\frac{\partial}{\partial s}(ur) + \frac{\partial}{\partial n}(vrh) = 0 \tag{3.3}$$

$$\frac{u}{h}\frac{\partial u}{\partial s} + v\frac{\partial u}{\partial n} + \frac{uvK}{h} = -\frac{1}{\rho h}\frac{\partial p}{\partial s} + \nu\{\frac{1}{h^2}\frac{\partial^2 u}{\partial s^2} + \frac{\partial^2 u}{\partial n^2} + \frac{1}{rh}\left[\frac{\partial}{\partial s}\left(\frac{r}{h}\right)\frac{\partial u}{\partial s} + \frac{\partial}{\partial n}(hr)\frac{\partial u}{\partial n}\right]\} \tag{3.4}$$

$$\frac{u}{h}\frac{\partial v}{\partial s} + v\frac{\partial v}{\partial n} - \frac{Ku^2}{h} = -\frac{1}{\rho}\frac{\partial p}{\partial n} + \nu\{\frac{1}{h^2}\frac{\partial^2 v}{\partial s^2} + \frac{\partial^2 v}{\partial n^2} + \frac{1}{rh}\left[\frac{\partial}{\partial s}\left(\frac{r}{h}\right)\frac{\partial v}{\partial s} + \frac{\partial}{\partial n}(hr)\frac{\partial v}{\partial n}\right]\} \tag{3.5}$$

where the geometric parameters $h = 1 + \frac{n}{R}$ and $K = \frac{1}{R}$ reflect longitudinal curvature effects whereas $r = r_0 + n\cos\theta$ accommodates the transverse curvature (cf. Figure 2).

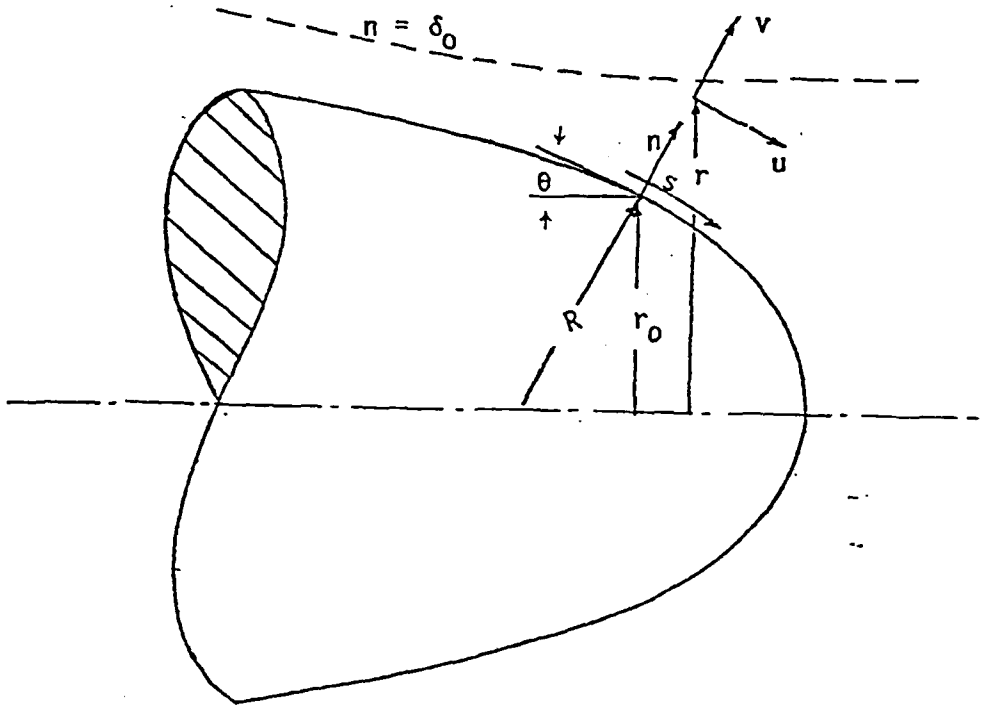

Figure 2. Coordinate system and geometric parameters where $r = r_o + n\cos\theta$, $r = r_o + n\cos\theta$, $\frac{d\theta}{ds} = -\frac{1}{R} = -K$, $\frac{\partial r}{\partial n} = \cos\theta$, $\frac{\partial r}{\partial s} = (1 + Kn)\sin\theta$, $\frac{dr_o}{ds} = \sin\theta$, and $h = 1 + Kn$.

The system of equations (3.3-3.5) can be simplified for distinct parts of the flow domain employing the relative order of magnitude analysis.

In region I of Fig. 2, the normal component of the velocity vector v is significantly smaller than the longitudinal component u. With this assumption, we introduce dimensionless variables that are of the order of unity in the boundary layer (cf. Van Dyke (1969)) as

$$\begin{aligned} &\tilde{u} = u/U \quad , \quad \tilde{v} = Re^{m}\ v/U \\ &\tilde{s} = s/L \quad , \quad \tilde{n} = Re^{m}\ n/L \\ &Re = UL/\nu \quad , \quad \tilde{p} = p/\rho\ U^2 \end{aligned} \tag{3.6}$$

Non-dimensionalization of the governing equations is achieved by inserting the dimensionless variables (3.6) into first the continuity equation (3.3).

$$\begin{aligned} &\frac{UL}{L}\frac{\partial}{\partial\tilde{s}}[(\tilde{r}_o + \tilde{n}\ Re^{-m}\cos\theta)u] + \frac{UL\ Re^{-m}}{L\ Re^{-m}}\ \frac{\partial}{\partial\tilde{n}}[(\tilde{r}_o + \tilde{n}\ Re^{-m}\cos\theta) \\ &*(1 + \tilde{K}\tilde{n}\ Re^{-m})\tilde{v}] = 0 \end{aligned} \tag{3.7}$$

$$\begin{aligned} &\frac{\partial}{\partial\tilde{s}}[(\tilde{r}_o + \tilde{n}\ Re^{-m}\cos\theta)u] + \frac{\partial}{\partial\tilde{n}}\{[\tilde{r}_o(1 + \tilde{K}\tilde{n}\ Re^{-m}) + \tilde{n}\ Re^{-m}\cos\theta]\tilde{v}\} \\ &+ Re^{-2m}\frac{\partial}{\partial\tilde{n}}[(\tilde{K}\tilde{n}^2\cos\theta)\tilde{v}] = 0\ . \end{aligned} \tag{3.8}$$

This equation after restoring original variables and rearrangement will reduce to

$$\frac{\partial}{\partial s}(r^j\ u) + \frac{\partial}{\partial n}[v(r^j - r_o^{\ j}(1-h^j))] + O(Re^{-2m}) = 0 \tag{3.9}$$

Substituting (3.6) into equation (3.4) yields:

$$\frac{U^2}{L}\frac{\tilde{u}}{1+\tilde{K}\tilde{n}\,Re^{-m}}\frac{\partial\tilde{u}}{\partial\tilde{s}}+\frac{U^2}{L}\tilde{v}\;\frac{\partial\tilde{u}}{\partial\tilde{n}}+\frac{U^2}{L}\;\frac{\tilde{K}\,Re^{-m}}{1+\tilde{K}\tilde{n}\,Re^{-m}}\;\tilde{u}\tilde{v}=$$

$$-\frac{U^2}{L}\frac{1}{1+\tilde{K}\tilde{n}\,Re^{-m}}\frac{\partial\tilde{p}}{\partial\tilde{s}}+\nu\{\frac{U}{L^2}\frac{1}{1+\tilde{K}\tilde{n}\,Re^{-m}}\frac{\partial^2\tilde{u}}{\partial\tilde{s}^2}+$$

$$(3.10)\qquad +\frac{U}{L^2}\;Re^{2m}\;\frac{\partial^2\tilde{u}}{\partial\tilde{n}^2}+\frac{U}{L^2}\frac{\partial\tilde{u}}{\partial\tilde{s}}\Big[\frac{1}{L(\tilde{r}_o+\tilde{n}\;Re^{-m}\cos\theta)(1+\tilde{K}\tilde{n}\,Re^{-m})^2}\frac{\partial\tilde{r}}{\partial\tilde{s}}$$

$$-\frac{1}{(1+\tilde{K}\tilde{n}\,Re^{-m})^3}\frac{\partial h}{\partial\tilde{n}}\Big]+\frac{U}{L^2}\;Re^{2m}\;\frac{\partial\tilde{u}}{\partial\tilde{n}}\Big[\frac{1}{L(\tilde{r}_o+\tilde{n}\;Re^{-m}\cos\theta)}\frac{\partial\tilde{r}}{\partial\tilde{n}}$$

$$+\frac{1}{(1+\tilde{K}\tilde{n}\,Re^{-m})}\frac{\partial h}{\partial\tilde{n}}\Big]\}\;.$$

Using the relation

$$\frac{1}{1+\varepsilon}=1-\varepsilon+\varepsilon^2+\cdots\qquad\frac{1}{1+\varepsilon}\approx 1-\varepsilon+O(\varepsilon^2)\;;\;\text{ where }\varepsilon\ll 1\;,$$

one can find for the previous equation

$$\tilde{u}\frac{\partial\tilde{u}}{\partial\tilde{s}}[1-\tilde{K}\tilde{n}\,Re^{-m}+O(Re^{-2m})]+\tilde{v}\frac{\partial\tilde{n}}{\partial\tilde{n}}+\tilde{K}\tilde{u}\tilde{v}\;Re^{-m}[1-\tilde{K}\tilde{n}\,Re^{-m}+O(Re^{-2m})]=$$

$$-\frac{\partial\tilde{p}}{\partial\tilde{s}}[1-\tilde{K}\tilde{n}\,Re^{-m}+O(Re^{-2m})]+\frac{\partial^2\tilde{u}}{\partial\tilde{s}^2}*Re^{-1}[1-2\tilde{K}\tilde{n}\,Re^{-m}+O(Re^{-2m})]+Re^{2m-1}\frac{\partial^2\tilde{u}}{\partial\tilde{n}^2}$$

$$(3.11)\qquad +\frac{\partial\tilde{u}}{\partial\tilde{s}}\Big\{\frac{Re^{-1}}{\tilde{r}_o L}[1-(\frac{\tilde{n}}{\tilde{r}_o}\cos\theta+2\tilde{K}\tilde{n})Re^{-m}+O(Re^{-2m})]$$

$$*\frac{\partial\tilde{r}}{\partial\tilde{s}}-Re^{-1}[1-3\tilde{K}\tilde{n}\;Re^{-m}+O(Re^{-2m})]\frac{\partial\tilde{h}}{\partial\tilde{s}}\Big\}$$

$$+\frac{\partial\tilde{u}}{\partial\tilde{n}}Re^{2m-1}\Big\{\frac{1}{\tilde{r}_o}[1-\frac{\tilde{n}}{\tilde{r}_o}\cos\theta\;Re^{-m}+O(Re^{-2m})]*\cos\theta\;Re^{-m}$$

$$+\tilde{K}\,Re^{-m}[1-\tilde{K}\tilde{n}\,Re^{-m}+O(Re^{-2m})]\Big\}$$

where

$$\frac{\partial \tilde{r}}{\partial \tilde{s}} = L\left[\frac{\partial \tilde{r}_o}{\partial \tilde{s}} + \tilde{n}\ Re^{-m}\ \frac{\partial \cos\theta}{\partial \tilde{s}}\right]$$

$$\frac{\partial \tilde{h}}{\partial \tilde{s}} = \tilde{n}\ Re^{-m}\ \frac{\partial \tilde{K}(s)}{\partial \tilde{s}}$$

After some rearrangements, the equation of motion in s-direction can be written as

$$\tilde{u}\frac{\partial \tilde{u}}{\partial \tilde{s}} + \tilde{v}\frac{\partial \tilde{u}}{\partial \tilde{n}} + Re^{-m}\left(-\tilde{K}\tilde{n}\tilde{u}\frac{\partial \tilde{u}}{\partial \tilde{s}} + \tilde{K}\tilde{u}\tilde{v}\right) = -\frac{\partial \tilde{p}}{\partial \tilde{s}}\left(1-\tilde{k}\tilde{n}\ Re^{-m}\right)$$

$$+ (Re)^{2m-1}\frac{\partial^2 \tilde{u}}{\partial \tilde{n}^2} + Re^{m-1}\frac{\partial \tilde{u}}{\partial \tilde{n}}\left(\frac{\cos\theta}{\tilde{r}_o} + \tilde{K}\right) + O(Re^{-1}, Re^{-m-1}, Re^{-2m}, \cdots) \tag{3.12}$$

Restoring the original variables in equation (3.12) will yield

$$(2-h^j)\ u\frac{\partial u}{\partial s} + v\frac{\partial u}{\partial n} + Kuv = -\frac{1}{\rho}(2-h^j)\frac{\partial p}{\partial s} + \nu\left\{\frac{\partial^2 u}{\partial n^2} + \frac{\partial u}{\partial n}\frac{\partial}{\partial n}\left[\left(\frac{r}{r_o}\right)^j + h^j\right]\right\} \tag{3.13}$$

Substituting (3.6) into equation (3.5) yields

$$\frac{U^2}{L}\frac{Re^{-m}}{(1+\tilde{K}\tilde{n}\ Re^{-m})}\tilde{u}\frac{\partial \tilde{v}}{\partial \tilde{s}} + \frac{U^2}{L}Re^{-m}\tilde{v}\frac{\partial \tilde{v}}{\partial \tilde{n}} - \frac{U^2}{L}\frac{\tilde{K}\tilde{u}^2}{(1+\tilde{K}\tilde{n}\ Re^{-m})} = -\frac{\rho U^2}{\rho L\ Re^{-m}}\frac{\partial \tilde{p}}{\partial \tilde{n}}$$

$$+ \nu\left\{\frac{Re^{-m}}{(1+\tilde{K}\tilde{n}\ Re^{-m})}\frac{U}{L^2}\frac{\partial^2 \tilde{v}}{\partial \tilde{s}^2} + \frac{U}{L^2}\frac{1}{Re^{-m}}\frac{\partial^2 \tilde{v}}{\partial \tilde{n}^2} + \frac{U}{L^2}Re^{-m}\frac{\partial \tilde{v}}{\partial \tilde{s}}\left[\frac{\partial}{\partial \tilde{s}}\left(\frac{\tilde{r}}{\tilde{n}}\right)\right]\right.$$

$$\left. + \frac{U}{L^2}\frac{1}{Re^{-m}}\frac{\partial \tilde{v}}{\partial \tilde{n}}\frac{\partial}{\partial \tilde{n}}(\tilde{r}\tilde{h})\right\} \tag{3.14}$$

Using again the relation $\frac{1}{1+\varepsilon} \approx 1-\varepsilon + O(\varepsilon^2)$ one obtains

$$Re^{-m}\left(1-\tilde{K}\tilde{n}\ Re^{-m}\right)\tilde{u}\frac{\partial \tilde{v}}{\partial \tilde{s}} + Re^{-m}\tilde{v}\frac{\partial \tilde{v}}{\partial \tilde{n}} - \tilde{K}\tilde{u}^2\left(1-\tilde{k}\tilde{n}\ Re^{-m}\right)$$

$$= -Re^{+m}\frac{\partial \tilde{p}}{\partial \tilde{n}} + Re^{-m-1}\left(1-2\tilde{K}\tilde{n}\ Re^{-m}\right)\frac{\partial^2 \tilde{v}}{\partial \tilde{s}^2} + Re^{m-1}\frac{\partial^2 \tilde{v}}{\partial \tilde{n}^2}$$

$$+ Re^{-m-1}\frac{\partial \tilde{v}}{\partial \tilde{s}}\left[\frac{\partial}{\partial \tilde{s}}\left(\frac{\tilde{r}_o + \tilde{n}\ Re^{-m}\cos\theta}{1+\tilde{K}\tilde{n}\ Re^{-m}}\right)\right]$$

$$+ Re^{m-1}\frac{\partial v}{\partial n}\left[\frac{1}{\tilde{r}_o}\left(\cos\theta\ Re^{-m} - \frac{\tilde{n}}{\tilde{r}_o}\cos\theta\ Re^{-m}\right) + \tilde{K}\ Re^{-m} + o(Re^{-2m})\right] \tag{3.15}$$

After rearrangements and simplifications, we have

$$
\begin{aligned}
&- \tilde{K}\tilde{u}^2\,Re^{-m} + Re^{-2m}\left(\tilde{u}\,\frac{\partial\tilde{v}}{\partial\tilde{s}} + \tilde{v}\,\frac{\partial\tilde{v}}{\partial\tilde{n}} + \tilde{K}^2\tilde{n}\,\tilde{u}^2\right) \\
&= -\frac{\partial\tilde{p}}{\partial\tilde{n}} + Re^{-1}\,\frac{\partial^2\tilde{v}}{\partial\tilde{n}^2} + Re^{-1-m}\,\frac{\partial\tilde{v}}{\partial\tilde{n}}\left(\frac{\cos\theta}{\tilde{r}_o} + \tilde{K}\right) + o(Re^{-m-1},\ Re^{-2m},\ \cdots)
\end{aligned}
\tag{3.16}
$$

Restoring the original variables yields

$$
K u^2 = \frac{1}{\rho}\frac{\partial p}{\partial n} + o(Re^{-1},\ Re^{-2m},\ \cdots)\ . \tag{3.17}
$$

Hence, for region I, (3.9, 3.13 and 3.17) are the basic equations where the flow indices i and j indicate the cases $i = j = 0$ for flow past a flat plate and $i = 1$, $j = 0$ for axisymmetric bodies with no longitudinal curvature and $i = 0$, $j = 1$ for flow without transverse curvature. Finally, $i = j = 1$ when longitudinal and transverse curvature effect exist. The exponent m is known for turbulent thin boundary layer flow with zero pressure gradient along a flat plate ($m = \frac{4}{5}$, see Schlichting, 1979, p. 638). Thus, terms of the order of Re^{-1}, Re^{-2m}, etc. are neglected.

Depending on the geometry of the submerged body it is possible that the boundary-layer thickness δ_o is not small (i.e. $\frac{n}{L} \approx O(1)$) but the mean flow streamlines still remain nearly parallel to the surface so that the normal component of the velocity v is still much smaller than the longitudinal component u. In this case, dimensionless variables that are of the order of unity in the boundary layer are introduced as:

$$
\begin{aligned}
\tilde{u} &= \frac{u}{U} \quad , & \tilde{v} &= \frac{Re^m\, v}{U} \\
\tilde{s} &= \frac{s}{L} \quad , & \tilde{n} &= \frac{n}{L} \\
Re &= \frac{UL}{\nu} \quad , & \tilde{p} &= \frac{p}{\rho U^2}
\end{aligned}
\tag{3.18}
$$

Inserting the dimensionless variables into the system (3.3-3.5), and following the same procedure that was used previously, one obtains

$$\frac{\partial}{\partial \tilde{s}}(\tilde{u}\tilde{r}) + Re^{-m}\frac{\partial}{\partial \tilde{n}}(\tilde{v}\tilde{h}\tilde{r}) = 0$$

$$\tilde{u}\frac{\partial \tilde{u}}{\partial \tilde{s}} + \tilde{h}\,Re^{-m}\,\tilde{v}\frac{\partial \tilde{u}}{\partial \tilde{n}} + \tilde{u}\tilde{v}\tilde{K} = -\frac{\partial \tilde{p}}{\partial \tilde{s}} + O(Re^{-1}) \tag{3.19}$$

$$Re^{-m}\,\tilde{u}\frac{\partial \tilde{v}}{\partial \tilde{s}} + \tilde{K}\tilde{u}^2 = -\frac{\partial \tilde{p}}{\partial \tilde{n}} + O(Re^{-2m}, Re^{-m-1}) .$$

Restoring the original variables

$$\frac{\partial}{\partial s}(ur) + \frac{\partial}{\partial n}(vhr) = 0$$

$$u\frac{\partial u}{\partial s} + hv\frac{\partial u}{\partial n} + uvK = -\frac{1}{\rho}\frac{\partial p}{\partial s} + O(Re^{-1}) \tag{3.20}$$

$$u\frac{\partial v}{\partial s} - Ku^2 = -\frac{1}{\rho}\frac{\partial p}{\partial n} + O(Re^{-2m}, Re^{-m-1})$$

For the turbulent flow analysis, time-averaged variables are denoted by overbars and random fluctuations by primes, so that

$$u = \bar{u} + u' \;,\; v = \bar{v} + v' \text{ and } p = \bar{p} + p' \tag{3.21}$$

where Reynolds stresses generated by the non-axisymmetric velocity fluctuations w' are neglected.

In addition, the following rules of operation for time-averaged variables are required for reference

$$\bar{\bar{f}} = \bar{f},\ \overline{f+g} = \bar{f} + \bar{g},\ \overline{f\cdot g} = \bar{f}\cdot\bar{g},\ \overline{\frac{\partial f}{\partial s}} = \frac{\partial \bar{f}}{\partial s} \text{ and } \overline{\int f ds} = \int \bar{f} ds$$

Hence, $u^2 = \bar{u}^2 + \overline{u'^2}$ and $\overline{u\cdot v} = \bar{u}\cdot\bar{v} + \overline{u'v'}$

Equations (3.22 to 3.24) contain five unknowns, namely, $\bar{u}$, $\bar{v}$, $\bar{p}$, $\overline{u'v'}$, $(\overline{u'^2})$. In order to gain closure it is therefore necessary to furnish some additional relationships.

Based on the objective of computational efficiency, and with the measured data sets found in the open literature, we postulate an algebraic turbulence or zero-equation model for the shear stresses reflecting curvature effects and relate these expressions directly to the normal stresses. Among the algebraic submodels, the mixing length hypothesis (MLH) has proven very useful and realistic for a wide range of case studies, provided that good choices were made for the mixing length distributions. However, the MLH cannot represent, in general, recirculating flows, turbulence convection or diffusion and non-zero effective viscosities or Prandtl numbers at the points of zero velocity gradients. Two commonly employed transport equations for turbulent shear stresses are the mixing length formula (Von Kármán (1931))

$$\overline{-u'v'} = \ell_m^2 \left|\frac{\partial u}{\partial y}\right| \frac{\partial u}{\partial y} \tag{3.27a}$$

and the eddy viscosity formula (Boussinesq (1877))

$$\overline{-u'v'} = \nu_t \frac{\partial u}{\partial y} \tag{3.27b}$$

where $\nu_t = \nu_t(\ell_m)$ again.

Following the method used for thin turbulent boundary layer calculations, a composite layer consisting of two regions is postulated (e.g. Baker & Launder (1974), Kwon & Pletcher (1979)). The distributions of ℓ_m and ν_t are then described by two separate empirical expressions. The criterion to define the inner and outer region of the boundary layer is the continuity of the eddy viscosity or the mixing length at the hypothetical "interface". The

shear stresses are a function of mean-time velocity and velocity gradient as well as mixing lengths which in trun are dependent upon the radii of curvatures, viz:

$$\overline{u'v'} = \overline{u'v'}\,[\nu_t(\ell_m, R, r_o);\ \bar{u}, \nabla\bar{u}]\,. \tag{3.28}$$

The turbulent flow analysis as well as predicted vs. measured results can be found in Eghlima (1982) and will be published in a forthcoming paper.

4. The governing equations for region II. In region II which possibly includes the point of separation, we can no longer assume that $v \ll u$. Hence, the flow in this region is characterized by strong interactions between the (detached) boundary layer and the outer potential flow. It is also conceivable that the attached (parabolic) boundary layer regime may be influenced by the (elliptic) reverse flow region after separation. Actual simulation results of thick separating boundary layer flows, viscid-inviscid interactions and near-wake effects will be discussed in a future series of papers. In this section we summarize the governing equations for region II.

After the appropriate correction in equation (3.6), since now $v \approx u$, and substitution into the system of equations (3.3 to 3.5) we obtain

$$\frac{\partial}{\partial s}(r^i u) + \frac{\partial}{\partial n}[v(r^i - r_o^i(1-h^j))] + O(Re^{-2m}) = 0 \tag{4.1}$$

$$u\frac{\partial u}{\partial s} + v\frac{\partial u}{\partial n} + uvK = -\frac{1}{\rho}\frac{\partial p}{\partial s} + \nu\frac{\partial^2 u}{\partial n^2} + O(Re^{-2m}) \tag{4.2}$$

$$u\frac{\partial v}{\partial s} + v\frac{\partial v}{\partial n} - Ku^2 = -\frac{1}{\rho}\frac{\partial p}{\partial n} + \nu\frac{\partial^2 v}{\partial n^2} + O(Re^{-2m}) \tag{4.3}$$

We note that transverse curvature effects only appear in the continuity equation (4.1); whereas the approximated s- and n-momentum equations (4.2 and 4.3) only explicitly contain the longitudinal curvature parameter in one term. However, in contrast to the first-order boundary layer equations, the Navier-Stokes equation in n-direction is almost fully preserved since $v \simeq u$. In addition, transverse curvature effects have to be coupled with the Reynolds stresses.

Again splitting the instantaneous variables into time-smoothed and random components we can derive the steady turbulent flow equations for region II as

$$\frac{\partial}{\partial s}\left(r_o^i \bar{u}\right) + \frac{\partial}{\partial n}\left(M \bar{v}\right) = 0 \tag{4.4}$$

$$\bar{u}\frac{\partial \bar{u}}{\partial s} + \bar{v}\frac{\partial \bar{u}}{\partial n} + \bar{u}\bar{v}K = -\frac{1}{\rho}\frac{\partial \bar{p}}{\partial s} + \nu\frac{\partial^2 u}{\partial n^2} - \frac{1}{M}\left[\left(\frac{M + r_o}{2}\right)\frac{\partial}{\partial s}\left(\overline{u'^2}\right) + \right.$$

$$\left. + \sin\theta\left(\overline{u'^2}\right) + \frac{\partial}{\partial n}\left(\overline{u'v'}\,M\right) + MK\left(\overline{u'v'}\right)\right] \tag{4.5}$$

$$u\frac{\partial \bar{v}}{\partial s} + \bar{v}\frac{\partial \bar{v}}{\partial n} - K\bar{u}^2 = -\frac{1}{\rho}\frac{\partial \bar{p}}{\partial n} + \nu\frac{\partial^2 \bar{v}}{\partial n^2} - \frac{1}{r_o}\left\{\frac{\partial}{\partial s}\left(\overline{u'v'}\,r_o\right) + \right.$$

$$\left. + \left(\frac{M + r_o}{2}\right)\frac{\partial}{\partial n}\left(\overline{v'^2}\right) + (\cos\Theta)\left(\overline{v'^2}\right) + K\,r_o\left[\left(\overline{v'^2}\right) - \left(\overline{u'^2}\right)\right]\right\} \tag{4.6}$$

where $M = r^j - r_o(1-h^j)$ and $K = \left(\frac{1}{R}\right)^{1/j}$.

The associated boundary conditions and the meaning of i and j are given in Section 3.

5. Case study for laminar boundary-layer flow with longitudinal curvature effect. To demonstrate the technical merit of the new governing equations, a spinoff from equation (3.4), the special case of laminar boundary layer flow with longitudinal curvature effects is analyzed. Van Dyke (1962), (1969) developed a higher-order boundary layer equation which takes into account the effect of longitudinal curvature as

$$u \frac{\partial u}{\partial s} + h^j v \frac{\partial u}{\partial n} + K u v = - \frac{1}{\rho} \frac{\partial p}{\partial s} + \nu h^j \frac{\partial^2 u}{\partial n^2} + \nu K \frac{\partial u}{\partial n} \tag{5.1}$$

In contrast, our s-momentum equation which can be directly obtained from (3.13) for $r_o \to$ reads

$$u \frac{\partial u}{\partial s} + h^j v \frac{\partial u}{\partial n} + K u v + [(1-h^j) u \frac{\partial u}{\partial s} + (1-h^j) v \frac{\partial u}{\partial n}] =$$
$$= - \frac{1}{\rho} \frac{\partial p}{\partial s} + \nu h^j \frac{\partial^2 u}{\partial n^2} + \nu K \frac{\partial u}{\partial n} + [-(1-h^j) \frac{1}{\rho} \frac{\partial p}{\partial s} + \nu(1-\bar{h}^j) \frac{\partial^2 u}{\partial n^2}]. \tag{5.2}$$

Hence, the proposed modeling equation (5.2) carries four additional terms which are of the same (second) order of magnitude when compared with equation (5.1). For h=1, which includes K=0, both equations reduce to Prandtl's boundary layer equation.

Before both equations are numerically compared it is of interest to trace the derivation procedures leading to the noted discrepancy. The traditional departure point for obtaining a higher-order approximation of laminar incompressible flow along a curved surface is either the system of equations (7) on page 119 in Goldstein (1948) or equations (22 and 23) on page 202 in Rosenhead (1963). The two sets of equations are mathematically equivalent but physical significance is lost when Goldstein's equation is multiplied by H (original notation) to generate Rosenhead's equation. Indeed, Rosenhead's

equation can be obtained in multiplying equation (3.4) by $h = 1 + \frac{n}{R}$ and then neglecting terms of the order of $(\frac{n}{R})^2$ and higher. During this procedure certain terms of the order of $(\frac{n}{R})$ could not be retained. This is best illustrated by considering an equation of the functional form

$$\frac{A}{h} + B\varepsilon + O(\varepsilon^2) + \cdots = 0 \tag{5.3a}$$

where $h \equiv 1 + \varepsilon + O(\varepsilon^2)$ and $\varepsilon \equiv \frac{n}{R}$.

Equation (5.3a) is representative for Goldstein's equation whereas Rosenhead's equation would take on the form

$$A + Bh\varepsilon + O(\varepsilon^2) + \cdots = 0 \tag{5.4a}$$

or

$$A + B\varepsilon + O(\varepsilon^2) + \cdots = 0. \tag{5.4b}$$

This last procedure, leading to Van Dyke's equation (5.1), indicates a shortcoming when compared with equation (5.3) now rewritten with $h^{-1} = (1+\varepsilon)^{-1} \approx 1-\varepsilon + O(\varepsilon^2)$

$$(1-\varepsilon)\, A + B\varepsilon + O(\varepsilon^2) + \cdots = 0. \tag{5.3b}$$

In equation (5.3b) which is representative of our equation (5.2), the term, $-\varepsilon A$, is preserved in the derivation procedure.

In Section 6, numerical results from a case study document the differences between equations (5.2) and (5.1).

6. Preparation of governing equations and numerical comparison. In order to simplify the comparison of numerical case studies, equations (3.23) and (3.24) are rewritten in a general form.

$$A_1\, u \frac{\partial u}{\partial s} + A_2\, v \frac{\partial u}{\partial n} + A_3\, uv = A_4 \frac{\partial p}{\partial s} + \nu A_5 \frac{\partial}{\partial n}\left(A_6 \frac{\partial u}{\partial n}\right) + \nu A_7 \frac{\partial u}{\partial n} \tag{6.1}$$

(6.2) $$A_3 u^2 = A_8 \frac{\partial p}{\partial n} + A_9 \frac{\partial u}{\partial n} \quad .$$

Now, Van Dyke's equation (5.1) is obtained by setting

$$A_1 = 1 \ , \ A_2 = h^j \ , \ A_3 = K \ , \ A_4 = -\frac{1}{\rho} \ , \ A_5 = h^j \ , \ A_6 = 1 \text{ and } A_7 = K \ .$$

Our s-momentum equation (5.2) requires

$$A_1 = 2 - h^j \ , \ A_2 = 1 \ , \ A_3 = K \ , \ A_4 = -(2-h)/\rho \ , \ A_5 = A_6 = 1 \text{ and } A_7 = K \ .$$

A finite difference method developed by H.B. Keller and described by Cebeci and Smith (1974) was selected after improvements were implemented as the best candidate for our modeling equations (Eghlima (1982)). In order to prepare the governing equations, submodels and boundary conditions for the numerical solution procedure, the following steps have to be accomplished: (1) transformation of the modeling equations into a new coordinate system (modified Mangler-Levy-Lee transformation), (2) transformation of the momentum equations and associated boundary conditions into a system of first-order partial differential equation, and (3) discretization of the modeling equations into finite difference forms using centered-differenced quotients. Some salient aspects of the first two steps are given below.

In order to remove the large variations of the boundary layer thickness and to obtain the governing equations (3.22 to 3.24) in simple form, an appropriate coordinate transformation is implemented.

(6.3a) $$d\xi = \rho_e \mu_t u_e \, ds$$

where, in general, the turbulence viscosity $\mu_t = \mu_e(1 + \varepsilon_m)$ and $\varepsilon_m = \varepsilon_m(\xi,\eta)$;

(6.3b) $$d\eta = [\rho_e u_e / \sqrt{2\xi}\,](\frac{r}{L_r})^j \, dn$$

In using the continuity equation (3.22), the stream function ψ can be defined as

(6.4a,b) $$u = \frac{1}{r^i \rho_e} \frac{\partial \psi}{\partial n} \qquad \text{and} \qquad v = -\frac{1}{M \rho_e} \frac{\partial \psi}{\partial s} \quad .$$

A dimensionless stream function $f(\xi,\eta)$ is related to $\psi(s,n)$ as:

(6.5) $$\psi(s,n) = \sqrt{2\xi}\, L_r^{\,i} f(\xi,\eta) \quad .$$

Now the partial-derivative operators $\left.\frac{\partial}{\partial s}\right|_n$ and $\left.\frac{\partial}{\partial n}\right|_s$ can be calculated. For example:

(6.6a) $$u = u_e f' \quad , \quad \text{where} \quad f' \equiv \frac{\partial f}{\partial \eta}$$

(6.6b) $$v = -\mu_e u_e \sqrt{2\xi}\, L_r^{\,i}/M \left[\frac{f}{2\xi} + \frac{\partial f}{\partial \xi} + \left(\frac{\partial \eta}{\partial \xi}\right)_n f' \right] .$$

Substituting the transformed variables and their derivatives into equations (3.23 and 3.24) - equation (3.22) is automatically satisfied - the momentum equations in the (ξ, η)- coordinate system read:

(6.7) $$[Q_1 f'']' + Q_2 f'f'' + Q_3 (f')^2 + Q_4 ff'' + Q_5 ff' + Q_6 f'' = Q_7 \left[\left(\frac{\partial p}{\partial \xi}\right)_\eta + \left(\frac{\partial \eta}{\partial \xi}\right)_n \left(\frac{\partial p}{\partial \eta}\right)_\xi \right] + Q_8 f' \frac{\partial f'}{\partial \xi} + Q_9 f'' \frac{\partial f}{\partial \xi} + Q_{10} f' \frac{\partial f}{\partial \xi}$$

(6.8) $$Q_{11} f'' + Q_{12} (f')^2 = Q_{13} \left(\frac{\partial p}{\partial \eta}\right)_\xi$$

where the Q's are functions of geometric, fluid, and flow parameters. In substituting $\left(\frac{\partial p}{\partial \eta}\right)_\xi$ from equation (6.8) into (6.7), a single equation results. To solve this third order, nonlinear partial differential equation with Keller's Box Method, new dependent variables $U(\xi,\eta)$ and $V(\xi,\eta)$ are introduced and a coupled system of first-order PDE's is generated:

(6.9a) $$f' = U = u/u_e$$

(6.9b) $$U' = V$$

(6.9c) $$[Q_1\ V]' + Q_2\ UV + Q_{14}(U)^2 + Q_4\ f\ V + Q_5\ f\ U + Q_{15}\ V = Q_7\ \left(\frac{\partial p}{\partial \xi}\right)_\eta + Q_8\ U\ \frac{\partial U}{\partial \xi} + Q_9\ V\ \frac{\partial f}{\partial \xi} + Q_{10}\ U\ \frac{\partial f}{\partial \xi}$$

The system (6.9) constitutes the new set of higher-order boundary layer equations for laminar and turbulent flows in region I.

The associated boundary conditions, formerly given as (3.25), can be written as:

(6.10a) $$f'(\xi,0),\ \text{i.e.}\ \ U(\xi,0) = 0\ \ \text{and}\ \ f(\xi,0) = 0.$$

In addition,

(6.10b) $$\eta \to \eta_\infty\ ,\quad f' \to \frac{1}{1 + D(\xi,\eta)}$$

where

$$D(\xi,\eta) = K\ \frac{r_o}{\cos\theta}\ \left[\left(1 + \frac{2L_r\ \cos\theta}{r_o^2}\ \frac{\sqrt{2\xi}}{\rho_e u_e}\ \eta\right)^{1/2} - 1\right].$$

For the case of flow past a flat plate, $D(\xi,\eta) = 0$ or $f' = 1$. The edge boundary condition may be sensitive to the specification of η_∞. To reduce this sensitivity, the expression (6.10b) is differentiated so that with

(6.10c) $$\eta \to \eta_\infty\ ,\quad f'' = -\ \frac{D_1(\xi,\eta)}{[1 + D(\xi,\eta)]^2}$$

where

$$D_1(\xi,\eta) = K\ \frac{2L_r\ \sqrt{2\xi}}{\rho_e u_e r_o}\ \left(1 + \frac{2L_r\ \cos\theta}{r_o^2}\ \frac{\sqrt{2\xi}}{\rho_e u_e}\ \eta\right)^{-1/2}$$

In combining (6.10b and c), the outer boundary-layer condition reads

(6.10d) $$\eta \to \eta_\infty\ ,\quad f'' + D_1(\xi,\eta)\ f'^2 = 0$$

or $$V + D_1 U^2 = 0.$$

The coefficients of (6.9c) are defined as

$$Q_{14} = Q_3 - Q_7 \frac{Q_{12}}{Q_{13}} \frac{\partial \eta}{\partial \xi} \quad , \quad Q_{15} = Q_6 - Q_7 \frac{Q_{11}}{Q_{13}} \frac{\partial \eta}{\partial \xi}$$

$$Q_1 = A_6 \left(\frac{r}{L_r}\right)^i \quad , \quad Q_2 = -\left(\frac{\partial \eta}{\partial \xi}\right)_n [Q_8 + Q_9]$$

$$Q_3 = -\frac{Q_8}{u_e} \frac{\partial u_e}{\partial \xi} - Q_{10} \frac{\partial \eta}{\partial \xi} \quad , \quad Q_4 = \frac{(L_r)^i}{M}$$

$$Q_5 = \frac{1}{A_5} \frac{K\sqrt{2\xi}}{\rho_e u_e} \left(\frac{L_r}{r}\right)^i Q_4 \quad , \quad Q_6 = \frac{A_7}{A_5} \frac{\sqrt{2\xi}}{\rho_e u_e}$$

$$Q_7 = -\frac{A_4}{A_1} \frac{Q_8}{u_e^2} \quad , \quad Q_8 = \frac{A_1}{A_5} 2\xi \left(\frac{L_r}{r}\right)^i$$

$$Q_9 = -2\xi Q_4 \quad , \quad Q_{10} = -2\xi Q_5$$

$$Q_{11} = A_9 \rho_e \left(\frac{r}{L_r}\right)^i \quad , \quad Q_{12} = -A_3\sqrt{2\xi}$$

$$Q_{13} = -A_8 \frac{\rho_e}{u_e} \left(\frac{r}{L_r}\right)^i \text{ and } A_7 \equiv G(s,n) = \frac{1}{(r_o)^i} \frac{\partial M}{\partial n} + \epsilon_m \left(\alpha \frac{h_j}{M} \sin\theta + \frac{1}{M} \frac{\partial M}{\partial n} + K\right).$$

For the simulation of (5.1) and (5.2), $G(s,n) = K$ where $r_o \to \infty$ and $\epsilon_m \equiv 0$, and the appropriate parameters A_1 to A_9 have to be inserted.

The boundary conditions for (5.1) and (5.2) are

$$U(\xi, \eta = 0) = 0 = f(\xi, \eta = 0) \text{ and } U(\xi, \eta - \eta_\infty) \to 1.$$

Following the procedure for implementing Keller's Box Method as outlined in Cebeci and Smith (1974), equations (6.9a-c) are programmed and then solved with an efficient, generalized equation solver developed by Varah (1976) and implemented by Flaherty and Mathon (1980). The pressure gradient is obtained from the solution of the inviscid flow regime (region III) for which the code developed by Cebeci et al. (1978) was employed.

To demonstrate the effect of longitudinal curvature and to show the numerical differences between equations (5.1) and (5.2), we selected an axisymmetric body designed and documented by Huang et al. (1979). Figure 3 depicts schematically one-half of the symmetric body which in our case is semi-infinite since $r_o \to \infty$. Of much higher resolution and physical interest is Fig. 4. It shows the local $\frac{\delta}{R} = K\delta$ vs. the chord length of the submerged body. The curve peaks early due to a sharp decrease of the radius of longitudinal curvature and then falls to zero (despite the growing boundary layer) when $R \to \infty$. When the flat middle section is over, $\frac{\delta}{R}$ increases again since R becomes finite and δ is quite thick ($\approx$ 0.4 ft) by then. The threshold value for $(\frac{\delta}{R})_o \approx 0.003$ was suggested by Cebeci and Smith (1974) based on Bradshaw's measurements which, however, were made for turbulent flows. For values $\frac{\delta}{R} > (\frac{\delta}{R})_o$ curvature effects become significant.

Figure 5 demonstrates that our "additional second-order terms" have indeed a significant effect, actually 10% at one point in this case study. It is evident that the maximal difference occurs after $\frac{\delta}{R}$ (x) has peaked. There are two reasons for this shift. Most influential is the term containing the pressure gradient which is retained in our derivation. In addition, there is an "after-effect" of the peak on the velocity distribution (enhanced by our four additional terms) which becomes fully visible a small distance downstream. The influential pressure gradient is about equal to zero at the maximum point for (CFA-CFV)/CFF which explains the sudden drop of the curve somewhat in correspondence with $\frac{\delta}{R}$ (x). Towards the tail of the body $\frac{\delta}{R}$ becomes significant again and, indeed, (CFA-CFV)/CFF $\neq$ 0.

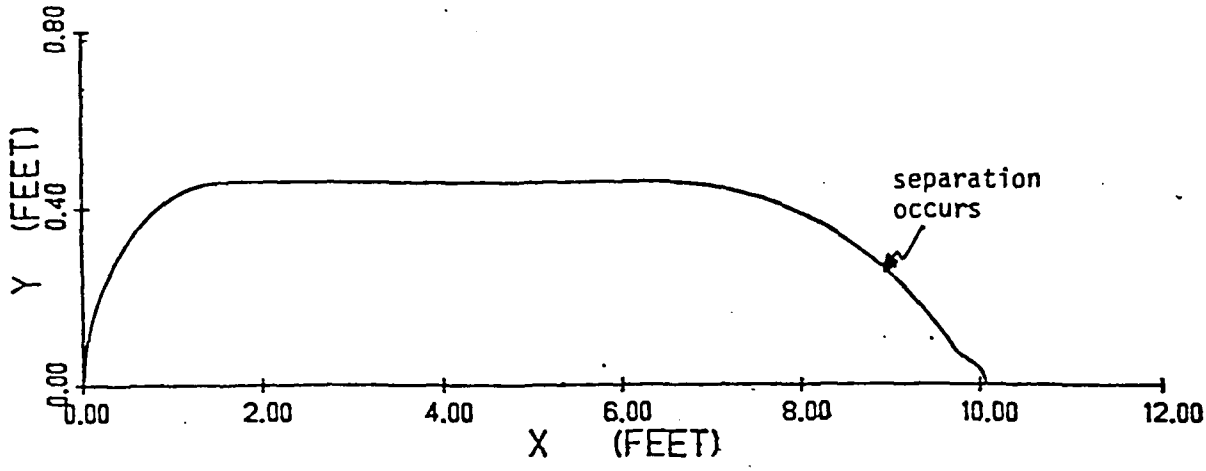

Fig. 3. Semi-infinite body with longitudinal curvature (adapted from Huang et al. 1980).

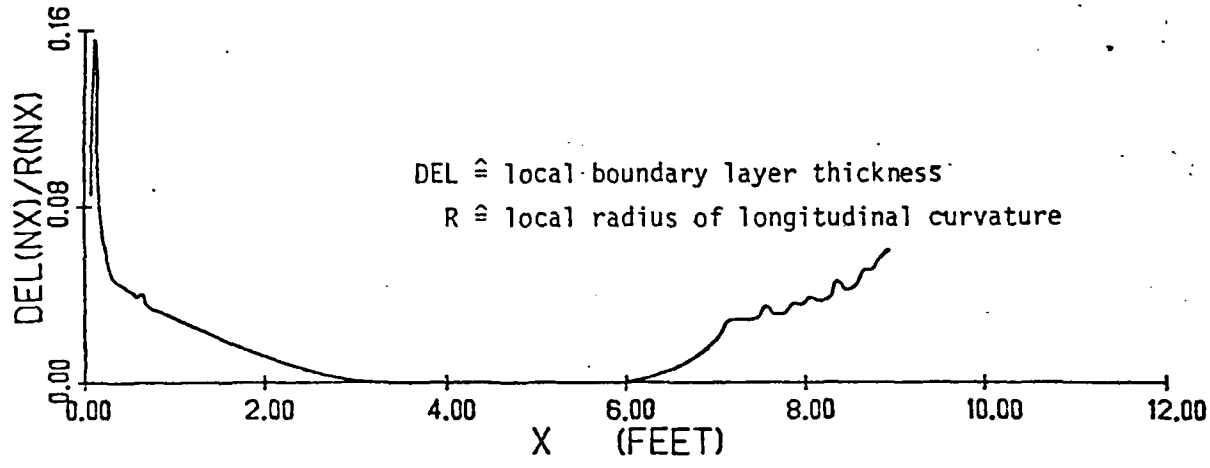

Fig. 4. Local $\frac{\delta}{R} = K\delta$ vs. chord length of submerged body.

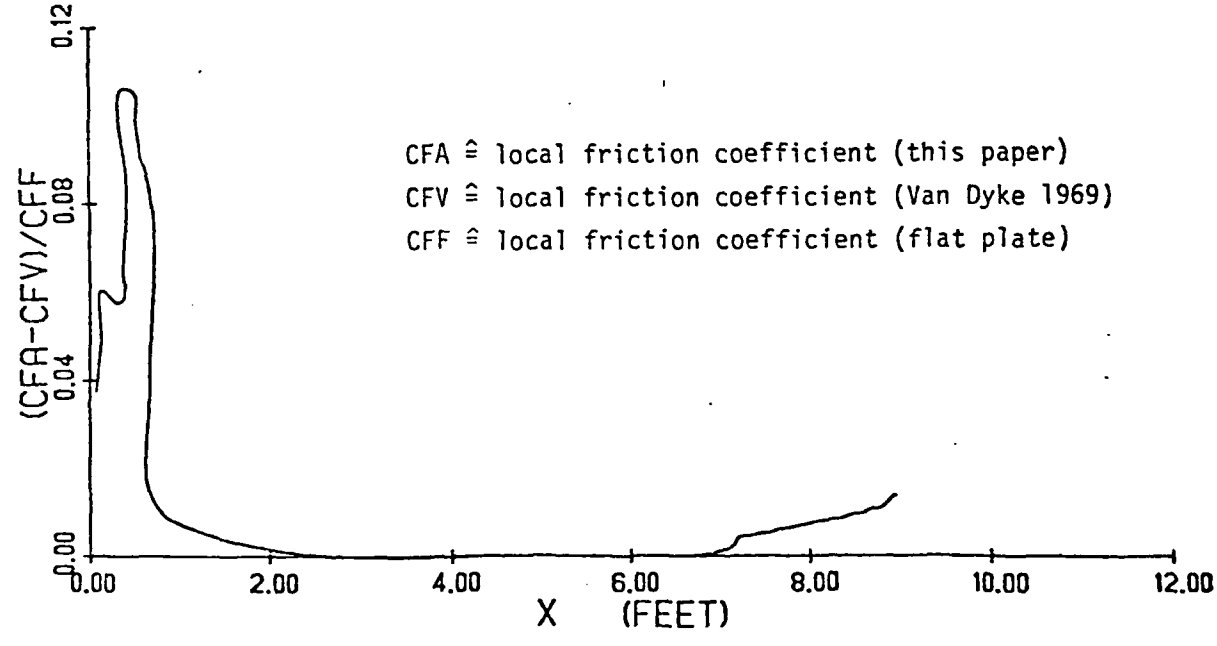

Fig. 5. Effects of thick laminar boundary layer development on the local friction coefficient: A comparison between equations (5.1) and (5.2) at Re ≈ $O(10^3)$.

In contrast to Fig. 5 where modeling improvements for points along the solid surface are shown, i.e. $\left.\frac{\partial u}{\partial y}\right|_{wall}(x)$, Figs. 6a-c depict the differences in boundary layer velocity profiles as produced by (5.1) and (5.2). Again, the higher accuracy of our equation is quite evident and has a significant effect on the local fluid flow parameters, especially near and at the wall, as well as on the point of separation. Figure 7 shows the development of the pressure gradient as discussed earlier.

7. Conclusions and future work. Based on a mathematically rigorous analysis, new sets of higher-order boundary layer equations for axisymmetric laminar and turbulent flow fields were derived. For the case of thick laminar boundary layer flow with longitudinal curvature effects, Van Dyke's momentum equation was numerically compared with our new equation which carries four additional (second-order) terms. The difference between the two equations in terms of local as well as integral properties of the flow system is significant. It is anticipated that the existing discrepancy between predicted and measured data for thick turbulent flows can now be closed with the use of the new higher-order boundary layer equations. Hence, several case studies will be conducted which will include the simulation of laminar and turbulent boundary layer developments along longitudinally and transversely curved surfaces and comparison with measured data sets published by So and Mellor (1973), Simpson et al. (1974) and Huang et al. (1979, 1980).

The turbulent flow data collected by Simpson et al. (1974) include separation. It is obvious that separating flows are very difficult to investigate. Strong interactions between the potential flow and thick turbulent boundary layer have to be accounted for. In addition, separation and near-wake effects might

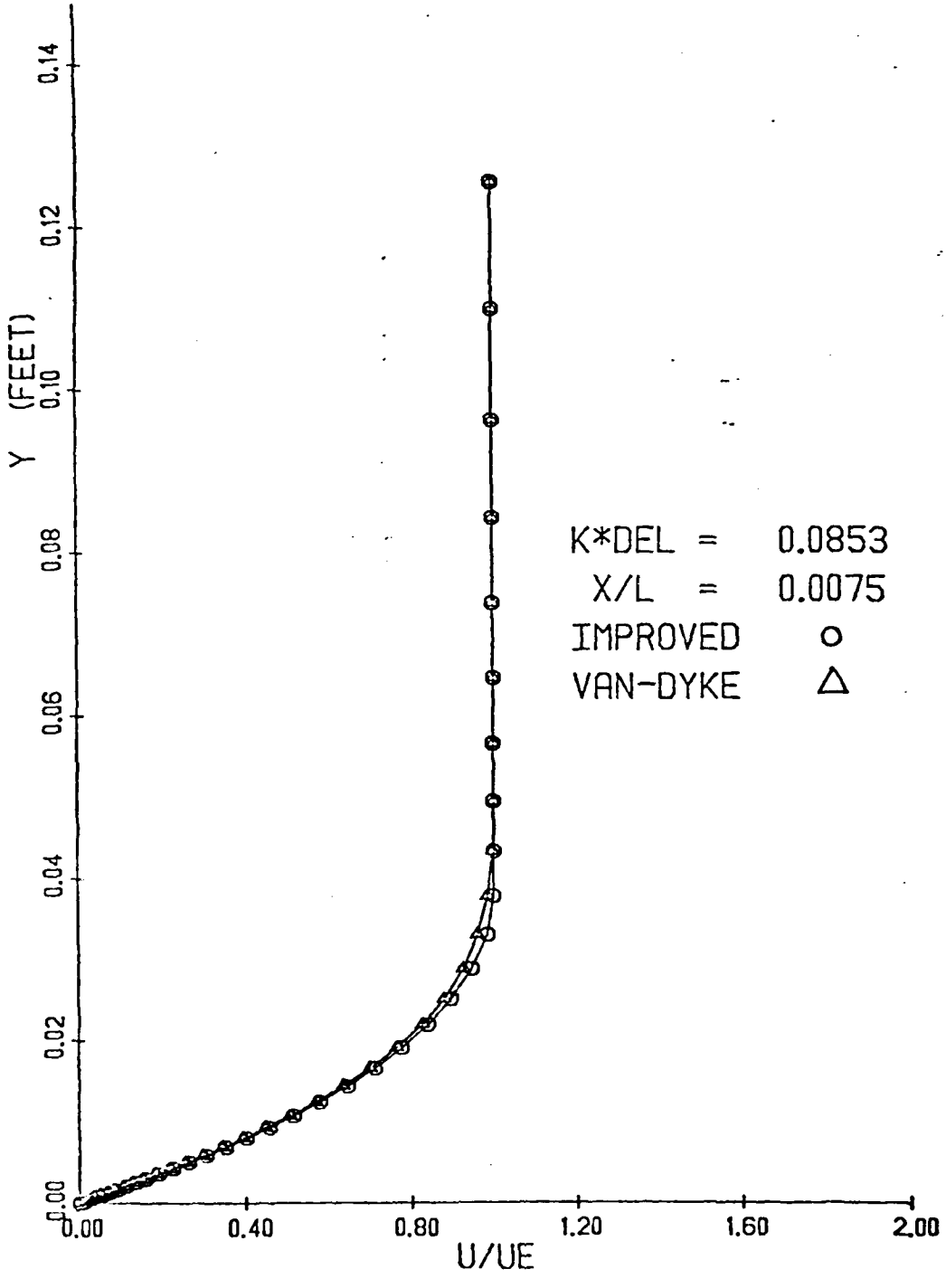

Fig. 6a: Comparison of laminar velocity profiles from (5.1) and (5.2) at the nose of the submerged body, i.e. before the peak of K*DEL

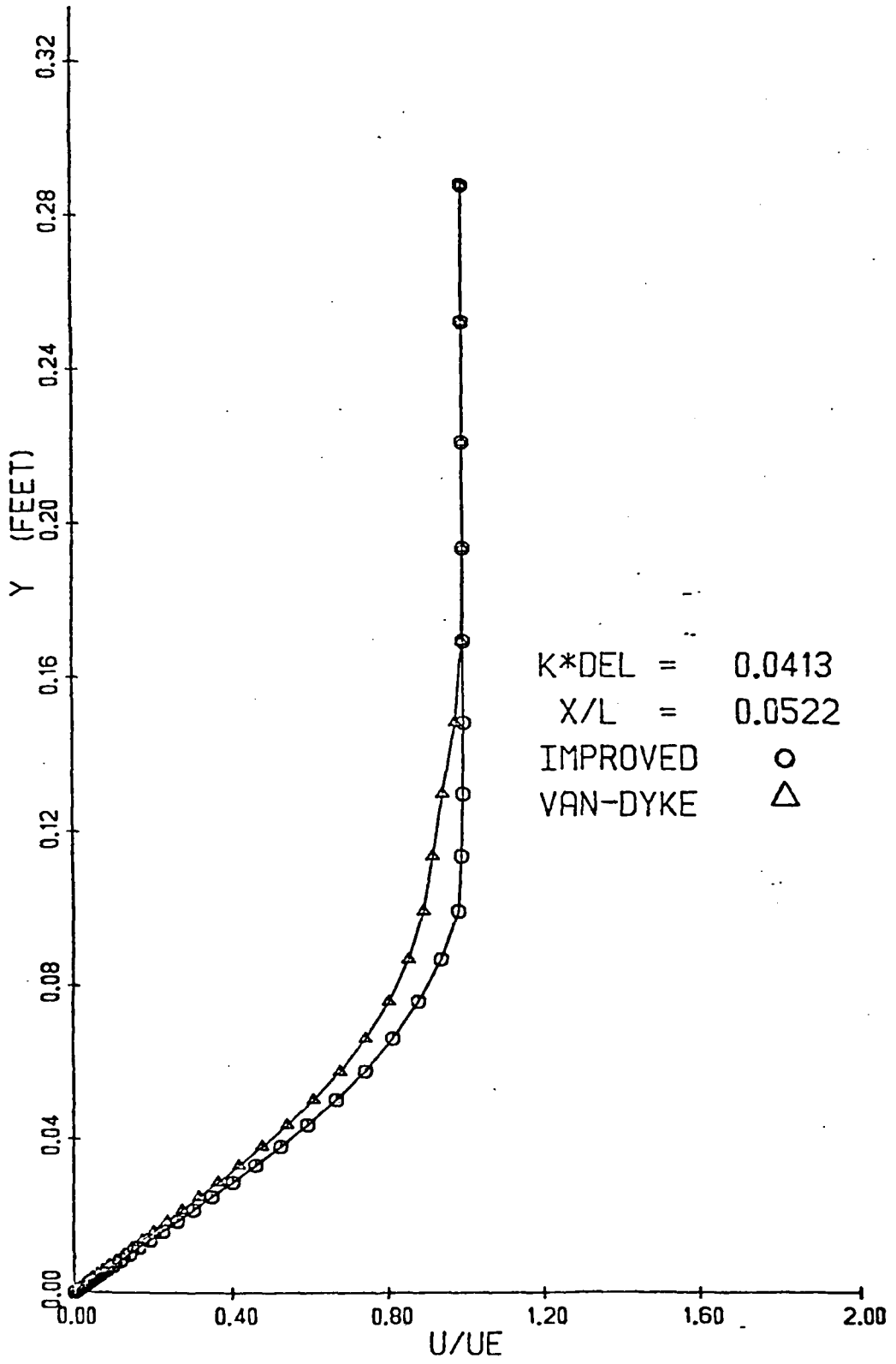

Fig. 6b: Comparison of laminar velocity profiles from (5.1) and (5.2) at the nose of the submerged body, i.e. after the peak of K*DEL and at $\left(\frac{\Delta c_f}{c_{fo}}\right)_{max}$ in Fig. 5.

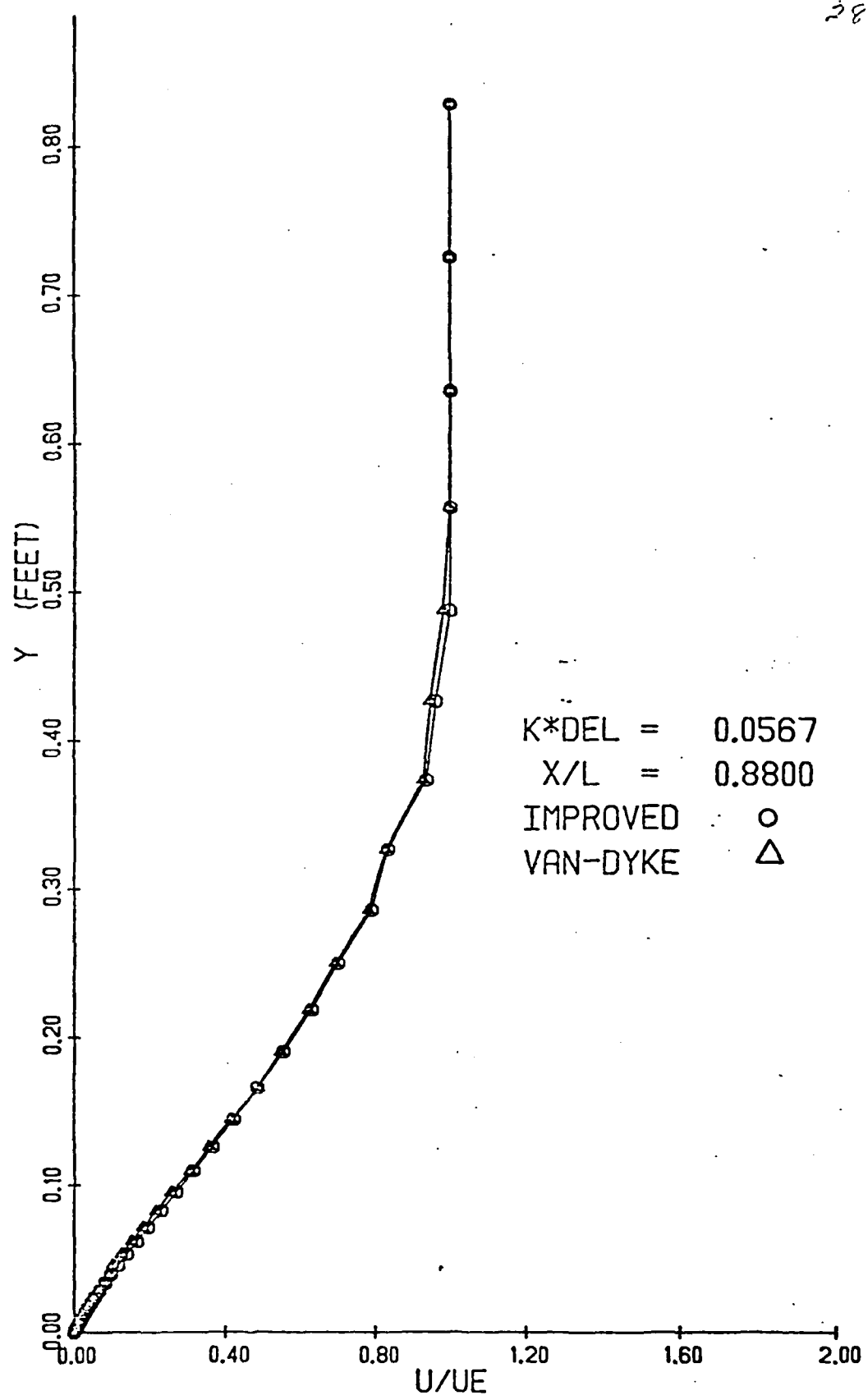

Fig. 6c: Comparison of laminar velocity profiles from (5.1) and (5.2) just before separation.

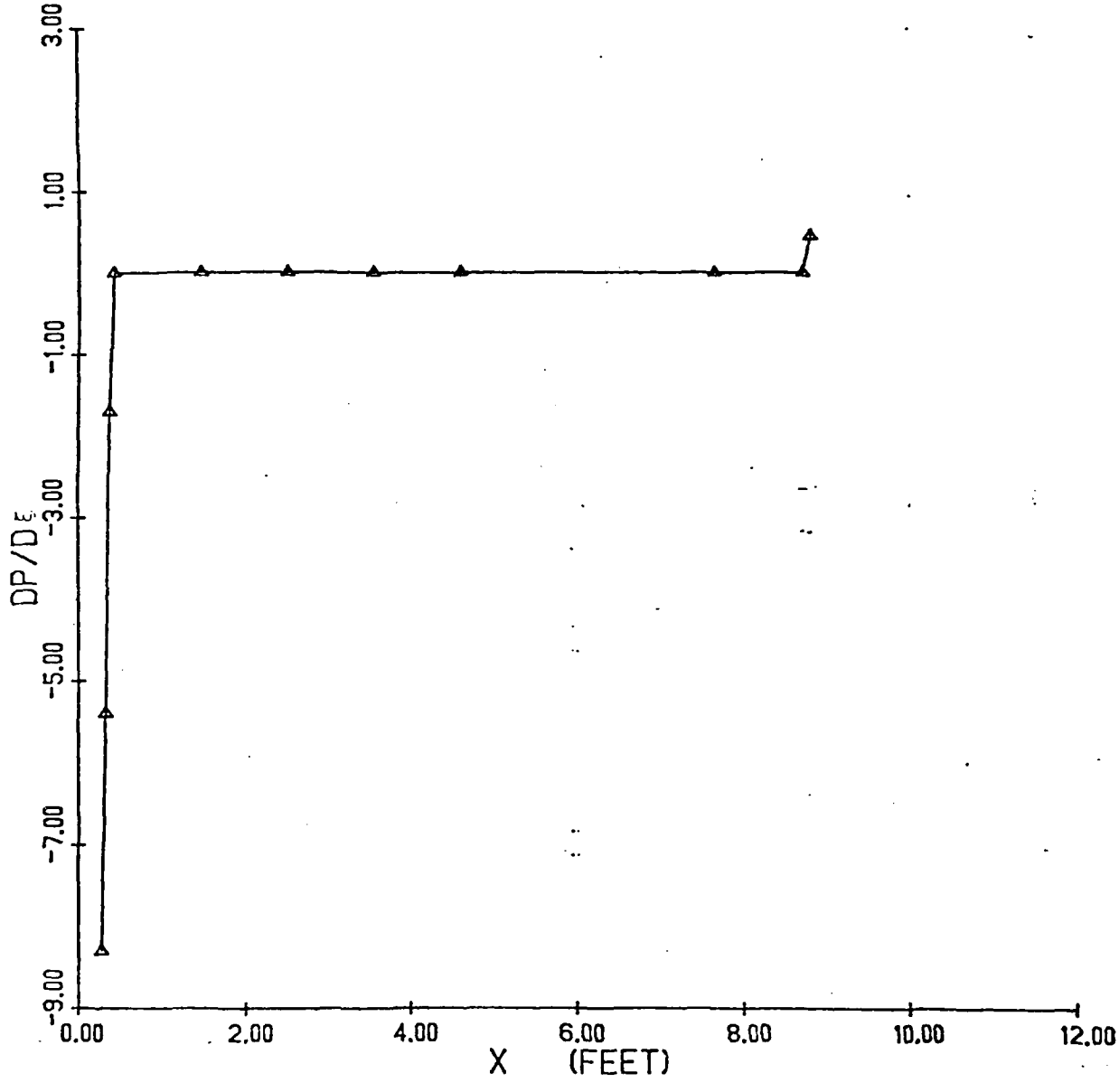

Fig. 7: Pressure gradient in s-direction vs. chord length of submerged body.

influence the upstream region of the still attached boundary layer. However, we will test the performance of our parabolic equations of region I also for regions containing mild recirculation so that the complex simulation of (4.4 to 4.6) can be avoided whenever possible.

In any case, only simple submodels for the Reynolds stresses will be employed in order to demonstrate also for turbulent flow the physical significance of our new equations. Previously, empirical turbulence models for specific case studies were used in conjunction with incomplete momentum equations to match laboratory observations.

To reduce the cumbersome and error-prone work of system discretization, the mesh generator developed by Kleinstreuer (1980) and advancements proposed by Dwyer et al. (1980) will be implemented for future case studies.

REFERENCES

R. J. BAKER AND B.E. LAUNDER (1974), Intern. J. Heat Mass Transfer, 17, pp. 275 and 293.

J. BOUSSINESQ (1877), *Théorie de l'écoulement tourbillant*, Mem. Pre. Par. Div. Sav., 23, Paris.

P. BRADSHAW (1973), *Effect of streamwise curvature on turbulent flows*, AGARDograph, No. 169.

_____ (1975), *Review: Complex turbulent flows*, J. F. Eng., Trans. ASME, pp. 146-154.

T. CEBECI (1971), *Wall curvature and transition effects in turbulent boundary layers*. AIAA Jour., 9, 1868.

T. CEBECI AND A. M. O. SMITH (1974) *Analysis of Turbulent Boundary Layers*, Academic Press, New York.

T. CEBECI, K. KAUPS, R. M. JAMES AND D. P. MACK (1978), *Boundary-layer and inverse potential - flow methods for axisymmetric bodies*, Report No. MDC J7895, Douglas Aircraft Company; prepared for ONR, Arlington, Virginia.

T. CEBECI, R. S. HIRSH AND J. H. WHITELAW (1979), *On the calculation of laminar and turbulent boundary-layers on longitudinally curved surfaces*, AIAA Journal, 17, 4.

S.C.R. DENNIS (1970), *Numerical solutions for steady flow past a circular cylinder at Reynolds number up to 100*, J. Fluid Mech., 42, p. 471.

H.A. DWYER, R.J. KEE AND B.R. SANDERS (1980), *Adaptive grid method for problems in fluid mechanics and heat transfer*, AIAA Journal, 18, p. 10.

A. EGHLIMA (1982), *Computation of Incompressible Turbulent Flow Fields with Non-Uniformities Including Separation Near the Tail of Axisymmetric Bodies*, Ph.D. thesis, Rensselaer Polytechnic Institute, Troy, New York (in preparation).

J.E. FLAHERTY AND W. MATHON (1980), *Collocation with Polynomial and Tension Splines for Singularly-Perturbed Boundary Value Problems*, Siam J. on Sci. Stat. Comput., Vol. 1, #2, p. 260-289.

J.E. FLAHERTY (1981) personal communication.

J.C. GILLIS AND J.P. JOHNSTON (1980), In: *Turbulent Shear Flows II*, L.J.S. Bradbury et al., eds, Springer-Verlag.

S. GOLDSTEIN (1948), *Modern Developments in Fluid Dynamics*, Oxford Press.

P.S. GRANVILLE (1978), *Similarity-law entrainment for thick axisymmetric turbulent boundary layer in pressure gradient*, J. Ship Res., 22, p. 131.

T.T. HUANG ET AL. (1979), *Stern boundary-layer flow on axisymmetric bodies*, 12th Symp. on Naval Hydrodynamics, Wash., D.C. (5-9 June 1978). Available from Nat. Acad. Sciences, Wash., D.C., p. 127.

_____ (1980), *Boundary-layer flow on an axisymmetric body with an inflected stern*, DTNSRDC-80/064.

H.B. KELLER AND H. TAKAMI (1966), *Numerical studies of steady viscous flow about cylinders*, Numerical Solutions of Nonlinear Differential Equations, D. Greenspan, ed., Wiley, New York.

C. KLEINSTREUER (1980), *Automized interactive mesh generators applicable as preprocessors of numerical models simulating flow systems*, Adv. Eng. Softw. J., CML Publications, 2, p. 5.

C. KLEINSTREUER (1982), *Mathematical Modeling of Engineering Systems*, Wiley-Interscience (In press).

O.K. KWON AND R.H. PLETCHER (1979), *Prediction of incompressible separated boundary layers including viscous-inviscid interaction*, Trans. ASME, J. Fluids Eng., 101.

J.H. MASLIYAH (1970), *Numerical study of steady flow past spheroids*, J. Fluid Mech., 44, p. 493.

R.N. MERONEY AND P. BRADSHAW (1975), *Turbulent boundary-layer growth over a longitudinally curved surface*, AIAA Journal, 13, p. 11.

V.C. PATEL (1974), A *simple integral method for the calculation of thick axisymmetric turbulent boundary layers*, Aeronaut. Quarterly, 25.

_____ (1974), *Measurement in the thick axisymmetric turbulent boundary-layer near the tail of a body of revolution*, J. Fluid Mech., 63.

V.C. PATEL AND Y.T. LEE (1978), *Thick axisymmetric boundary layers and wakes: Experiment and theory*, Paper 4, Int'l. Symp. on Ship Viscous Resistance, Göteborg, Sweden.

V.C. PATEL AND D.H. CHOI (1980), In: *Turbulent Shear Flows II*, L.J.S. Bradbury et al., eds., Springer Verlag.

S.B. POPE AND J.H. WHITELAW (1976), *The calculation of near-wake flows*, J. Fluid Mech., 73, p. 9.

B.R. RAMAPRIAN AND B.G. SHIVAPRASD (1978), *The structure of turbulent boundary-layer along mildly curved surfaces*, J. Fluid Mech., 85, p. 273.

A.K. RASTOGI AND J.H. WHITELAW (1971), *Procedure for predicting the influence of longitudinal curvature on boundary-layers*, ASME Paper 71-WA/FE-37.

J.J. RILEY AND R.W. METCALFE (1980), In: *Turbulent Shear Flows II*, L.J.S. Bradbury et al., eds., Springer-Verlag.

L. ROSENHEAD (1963), *Laminar Boundary Layers*, Clarendon Press, Oxford.

H. SCHLICHTING (1979), *Boundary Layer Theory*, McGraw-Hill, New York.

R.L. SIMPSON ET AL. (1974), *Laser and hot-film anemometer measurements in a separating turbulent boundary layer*, Tech. Rep. WT-3, Southern Methodist Univ., Dallas, Texas.

F.T. SMITH (1979), *Laminar flow of an incompressible fluid past a bluff body: the separation, reattachment, eddy properties and drag*, J. Fluid Mech., 92, p. 171.

A.J. SMITH, S.T. YOUNG AND P. BRADSHAW (1979), *The effect of short regions of high surface curvature on turbulent boundary-layer*, J. Fluid Mech., 92, p. 209.

R.M.C. SO AND G. MELLOR (1973), J. *Fluid Mech.*, 60, p. 43.

J.S. SON AND T.J. HANRATTY (1969), *Numerical solution for flow around a cylinder at Reynolds numbers of 40, 200 and 500*, J. Fluid Mech., 35, p. 369.

M. VAN DYKE (1962), *Higher approximation in boundary-layer theory. Part I. General Analysis*, J. Fluid Mech., p. 161.

M. VAN DYKE (1969), *Higher order boundary-layer theory*, Ann. Rev. Fluid Mech., p. 265.

K.M. VARAH (1976), *Alternate Grow and Column Elimination for Solving Certain Linear Systems*, Siam J. Numer. Anal., Vol. 13, p. 71-75.

T.H. VON KÁRMÁN (1931), *Mechanische Ähnlichkeit und Turbulenz*, Proc. 3rd Int. Congress Appl. Mech., Stockholm, Part 1, p. 85.

J.C. WILLIAMS III (1977), *Incompressible boundary layer separation*, Ann. Rev. Fluid Mech., 9, p. 113.

F.M. WHITE (1974), *Viscous Fluid Flow*, McGraw-Hill, New York.

Th.Y. WU (1972), *Cavity and wake flows*, Ann. Rev. Fluid Mech., No. 8025, p. 243.

NOMENCLATURE

A_1 to A_9	parameters in equations (6.1 & 6.2)
f	dimensionless stream function defined by Eq. (6.5)
$h_1 \equiv h = 1 + Kn$	metric coefficient (dimensionless)
$h_2 = 1$	metric coefficient (dimensionless)
$h_3 = r$	metric coefficient (dimensionless)
$K = \frac{1}{R}$	longitudinal curvature $(ft)^{-1}$
L_r	reference length (ft)
ℓ_m	mixing length (ft)
$M = (r)^i - (r_o)^i [1 - (h)^j]$	(ft)
n	coordinate, normal to body (ft)
P	pressure
$\bar{p}$	non-dimensional pressure
Q_1 to Q_{15}	parameters in equation (6.9c)
R	radius of longitudinal curvature (ft)
$r = r_o + n \cos\theta$	transverse radius of curvature (ft)
r_o	transverse radius of curvature of the body (ft)
s	coordinate along the body surface (ft)
$\bar{s}$	non-dimensional coordinate along the body surface
t	time
u	$\underline{s}$ component of the velocity (ft/sec)
$\tilde{u}$	dimensionless velocity in $\underline{s}$ direction
$\bar{u}$	time-averaged velocity in $\underline{s}$ direction (ft/sec)
u'	velocity fluctuation in $\underline{s}$ direction (ft/sec)
$\bar{u'^2}$	Reynolds normal stress in $\underline{s}$ direction

$U \equiv \frac{\partial f}{\partial \eta}$	dimensionless variable
U_{inf}	free stream velocity
v	$\underline{n}$ component of the velocity (ft/sec)
$\tilde{v}$	dimensionless velocity in $\underline{n}$ direction
$\bar{v}$	time-averaged velocity in $\underline{n}$ direction (ft/sec)
v'	velocity fluctuation in $\underline{n}$ direction (ft/sec)
$\bar{v}'^2$	Reynolds normal stress in $\underline{n}$ direction
$V \equiv \frac{\partial U}{\partial \eta}$	non-dimensional variable
w	velocity normal to (s-n) plane (ft/sec)
$\bar{w}'^2$	Reynolds normal stress normal to (s-n) plane
$\overline{u'v'}$	Reynolds shear stress

Greek Symbols

β	longitudinal curvature effect parameter
θ	angle between axis of symmetry and tangent to the surface (radiant)
ν	kinematic viscosity
ν_t	eddy viscosity
μ	dynamic viscosity (lbm/ft-sec)
ρ	mass density (lbm/ft^3)
ξ	transformed s-coordinate (lbm/ft-sec)

η	transformed n-coordinate (non-dimensional)
δ	boundary-layer thickness (ft)
$\epsilon_m = \frac{\nu_t}{\nu}$	non-dimensional eddy viscosity

Superscripts

i	transverse curvature index =1 does exist =0 does not exist
j	longitudinal curvature index =1 does exist =0 does not exist

Subscripts

e	outer edge of boundary layer
eff	effective value
f	flat plate
t	turbulent
w	wall

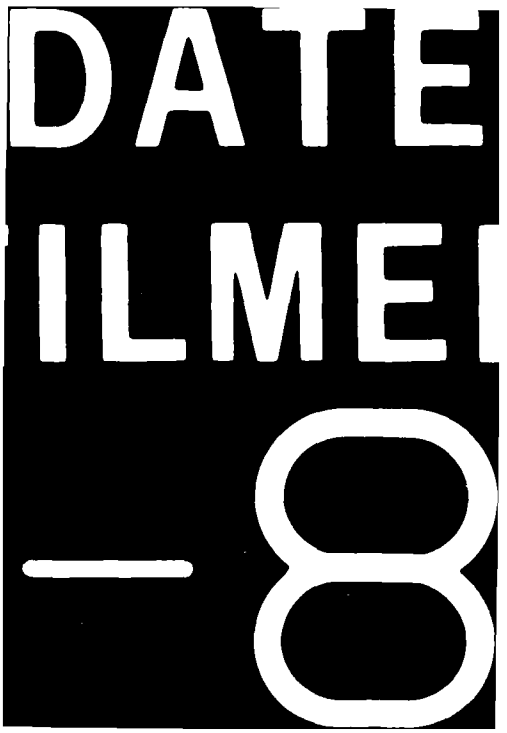
DATE
ILME
8